



HAL
open science

Single-crystal growth, structure, and optical properties of a new non-centrosymmetric germanate, $\text{RbSbGe}_3\text{O}_9$

Pascale Armand, M. Tillard, A. Haidoux, L. Daenens

► **To cite this version:**

Pascale Armand, M. Tillard, A. Haidoux, L. Daenens. Single-crystal growth, structure, and optical properties of a new non-centrosymmetric germanate, $\text{RbSbGe}_3\text{O}_9$. *Journal of Solid State Chemistry*, 2020, 286, pp.121290. 10.1016/j.jssc.2020.121290 . hal-02995228

HAL Id: hal-02995228

<https://cnrs.hal.science/hal-02995228>

Submitted on 9 Nov 2020

HAL is a multi-disciplinary open access archive for the deposit and dissemination of scientific research documents, whether they are published or not. The documents may come from teaching and research institutions in France or abroad, or from public or private research centers.

L'archive ouverte pluridisciplinaire **HAL**, est destinée au dépôt et à la diffusion de documents scientifiques de niveau recherche, publiés ou non, émanant des établissements d'enseignement et de recherche français ou étrangers, des laboratoires publics ou privés.

Single-crystal growth, structure, and optical properties of a new non-centrosymmetric germanate, $\text{RbSbGe}_3\text{O}_9$

P. Armand*, M. Tillard, A. Haidoux, L. Daenens

ICGM, Université de Montpellier, CNRS, ENSCM, Montpellier, France

Corresponding author

*E-mail : pascale.armand@umontpellier.fr; Tel : +33 (0)4 67 14 33 19

ORCID : 0000-0001-8921-5427.

Abstract

The $\text{RbSbGe}_3\text{O}_9$ compound, grown by the high-temperature solution technique from the $\text{Rb}_2\text{Mo}_4\text{O}_{13}$ flux, crystallizes in the trigonal non-centrosymmetric space group $P31c$ ($n^\circ. 159$). The structure was solved and refined from single-crystal X-ray diffraction data recorded at ambient temperature, $a = 12.1378(2)$, $c = 9.9553(2)$ Å, $V = 1270.18(5)$ Å³, $RI = 0.0241$ and $wR2 = 0.0452$ for all data. The unit cell contains six formula units. The three-dimensional $\text{RbSbGe}_3\text{O}_9$ network is built with three-membered units $[\text{Ge}_3\text{O}_9]^{6-}$ of regular germanate tetrahedra involving three independent Ge atoms. The Ge_3O_3 central rings located in the ab plan deviate only slightly from the planarity. Antimony Sb^{V} is octahedrally coordinated by oxygen, and rubidium (Rb^+), which is surrounded by six oxygen atoms, is located in the channels of the 3-D network. The structure of $\text{RbSbGe}_3\text{O}_9$ containing both isolated SbO_6 octahedra and Ge_3O_9 cyclic units is comparable but not isostructural to the benitoite type. The almost flat character of the Ge_3O_3 rings is also attested by the vibrational study at room temperature via non-polarized infrared and Raman spectroscopy.

KEYWORDS: A. oxides, B. crystal growth, C. X-ray diffraction, C. Raman spectroscopy, D. crystal structure

1. INTRODUCTION

Since non-polar and non-centrosymmetric single-crystals are potential candidates for integrating devices in the fields of piezoelectric and/or nonlinear optical applications, the development of new compositions is still current. For many years, we have been interested in the germanate family with the development and the characterizations of the GeO_2 single-crystal with the α -quartz structure [1-4]. Our researches are now focused on the benitoite-type family and especially on the compounds of general formula MXGe_3O_9 where M is a monovalent or bivalent chemical element with a large size (K, Rb, Ba, Ca, Tl) and X is a tetravalent or pentavalent element which can adopt an octahedral coordination (Sn, Nb, Ti, Ta, Zr) [5-11]. These non-centrosymmetric oxides present a mixed framework built with XO_6 octahedra and GeO_4 tetrahedra, the latter forming a 3-membered ring anion $[\text{Ge}_3\text{O}_9]^{6-}$ with the local high symmetry D_{3h} [5,6,9].

Very few cyclogermanate compounds with a benitoite-like structure have been identified and, for the majority, it is indicated in the literature that they were obtained in the form of powder or ceramic [5-11]. This is why it seemed important to us to develop new germanate compositions and to obtain them as single-crystals.

This paper reports on the crystal-growth using the flux method of the new cyclogermanate $\text{RbSbGe}_3\text{O}_9$, and its structure determination using single-crystal X-ray diffraction data registered at room-temperature. The optical properties of the as-grown crystal, investigated through infrared and Raman spectroscopies, are also discussed.

2. EXPERIMENTAL SECTION

2.1 Single-crystal growth.

The slow-cooling method of the high-temperature solution growth technique was used to spontaneously nucleate $\text{RbSbGe}_3\text{O}_9$ crystals. First, a glass from the GeO_2 - $\text{SbO}_{1.5}$ binary-system was prepared, from the starting materials Sb_2O_3 and GeO_2 mixed in the Sb/Ge molar ratio of 0.33, to be used as the solute. This mixture was heated above its melting temperature in a platinum crucible, held two hours for homogenization and ice-quenched to room-temperature. The $\text{Rb}_2\text{Mo}_4\text{O}_{13}$ compound ($T_f = 530^\circ\text{C}$), chosen as the flux, was synthesized from Rb_2CO_3 and MoO_3 via a solid-state reaction at 450°C during two weeks.

For the high-temperature flux growth experiments, the glass solute was thoroughly mixed with the flux respecting a solute-to-flux ratio of 10/90 in weight. A charge of 20 g of this mixture was placed in a 25 cm^3 platinum covered crucible, heated up to 970°C and kept for 12 h at this temperature without mechanical rotation. Then, the melted charge was slowly cooled down to 745°C at the rate of $1^\circ/\text{hr}$. The growth experiment yielded colorless crystals with quality and size suitable for single-crystal X-ray structure determination and vibrational characterizations.

2.2 Single-crystal X-ray collection.

A small platelet was selected for X-ray experiments using a stereomicroscope equipped with a polarizing filter. The room-temperature diffracted intensities were collected on a Bruker D8 Venture 4-circle diffractometer equipped with an Incoatec $\text{I}\mu\text{S}$ 3.0 Mo micro-source ($110\ \mu\text{m}$ beam, $\text{MoK}\alpha$ radiation) and a Photon II CPAD detector. The data collection and the cell refinement were performed with the Apex software suite [12] also used for data reduction, intensity scaling and correction for Lorentz and polarization effects. Absorption correction was applied using the multi-scan method (SADABS).

The structure was solved and further refined on F^2 by the full-matrix least-squares method provided in the SHELXTL software package [13,14].

The atomic positions and the anisotropic displacement parameters have been refined for all the atoms. The entire filling of the atomic sites has been checked by the free refinement of the occupational factors which did not deviate from unity within the standard deviation limits.

2.3 Characterizations.

The X-ray powder diffraction experiment was performed at room temperature using an X'Pert Pro II diffractometer (PANalytical) equipped with a dichromatic Cu $K\alpha$ radiation and a CCD detector. Scanning step width of 0.033° in 2θ and scanning rate of 400 s/point were used to record the patterns in the 2θ range from 10 to 80° .

EDX analyses were set up on a Quanta 200 FEG (FEI) Scanning Electron Microscopy (SEM) equipped with an SDD diode as the detector (Oxford INCA). Spectra were registered under a low vacuum (around 10^{-3} Pa) at 15 kV.

The room-temperature Fourier Transform Infrared transmission (FTIR) spectrum was registered via the KBr method (KBr salt transparent to the infrared light), in the air using an IFS 66v spectrometer (Bruker) supplied with a detector MCT. The resolution is ± 4 cm^{-1} .

The non-polarized Raman spectrum was recorded at room temperature in 180° backscattering geometry, using the 473 nm excitation line of a blue diode laser, on a Horiba Jobin-Yvon LabRam Aramis confocal spectrometer equipped with an Olympus optical microscope and a Peltier-cooled charge-coupled device (CCD). The spectral resolution accuracy is of the order of ± 2 cm^{-1} .

The differential scanning calorimetry (DSC) experiment was carried out using a NETZSCH STA 449F1 equipment, in the air, with a heating rate of $5^\circ/\text{min}$ from ambient temperature to 1200°C .

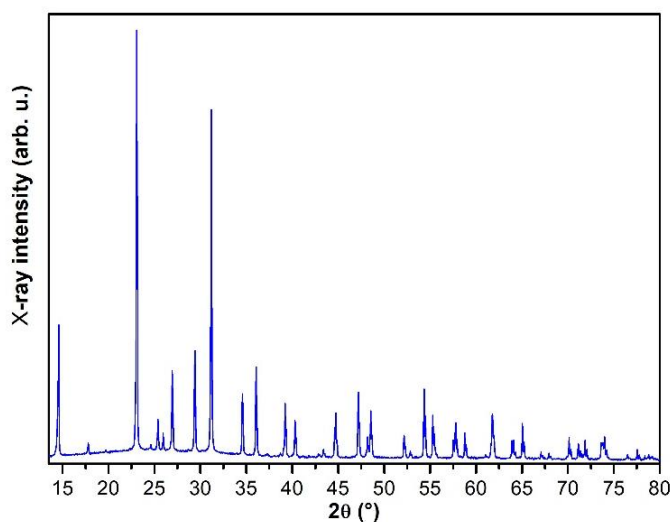
3. RESULTS AND DISCUSSION

3.1. Crystal growth

Via spontaneous nucleation from the high-temperature flux method, visually transparent and colorless as-grown crystals with a micro-meter size were obtained. These crystals display platy and hexagonal-shaped geometries. Only the Ge, Rb and Sb contents were detected via EDX chemical analysis, they were found in the atomic proportions Rb/Sb of 1 and Ge/Sb of 3. No significant variation in the composition was noticed from at least three microprobe analyses across the crystal. This result agrees with the nominal $\text{RbSbGe}_3\text{O}_9$ stoichiometric composition.

The DSC measurement, from room-temperature to 1200°C with a $5^\circ/\text{min}$ heating rate, has shown a unique exothermic thermal event occurring at $1061 \pm 1^\circ\text{C}$ (maximum of the peak). This means that the compound $\text{RbSbGe}_3\text{O}_9$ is thermally stable up to $\cong 1010^\circ\text{C}$ and does not undergo a structural transformation up to this temperature.

The θ - 2θ X-ray powder diffraction pattern recorded for $\text{RbSbGe}_3\text{O}_9$ is shown in Figure 1. Most of the reflections can be indexed based on the JCPDS card number 00-027-0524 [15] which mentions a hexagonal system with $P\bar{6}c2$ space group (n°. 188) and cell constants $a = 7.0008$, and $c = 9.9402 \text{ \AA}$. However, some small reflections occurring in the 2θ range from 20



to 25° are not taken into account.

Figure 1: Room-temperature X-ray powder diffraction pattern of RbSbGe₃O₉ sample.

3.2. Structure determination, and description.

Indexation of the reflections recorded for the single-crystal of RbSbGe₃O₉, in such a unit cell of dimensions $a = 7.0$, $c = 9.94$ Å would require to disregard too many diffraction spots. To take into account the whole diffraction spots, a larger primitive lattice must be considered. This choice is also supported by the entire indexation of the X-ray powder pattern, given in Figure 1, in a trigonal $P31c$ cell of parameters $a = 12.1378(2)$ and $c = 9.9553(2)$ Å, using the profile fitting procedure of Jana2006 [16]. The statistical tests on the diffracted intensities indicate a non-centrosymmetric space group. The extinction conditions are compatible with the symmetry $P31c$ and the structure solution found in this space group could be refined to 3.4 %. The occurrence of twinning was confirmed during the final steps of the refinement and the consideration of the twin law $[0\ 1\ 0\ 1\ 0\ 0\ 0\ 0\ -1]$ led to an additional improvement in the agreement factor which finally converges to $R1 = 2.07$ %.

The crystal data and the refinement parameters are reported in Table 1 while the atomic positions and displacement parameters are listed in Table 2. Supplementary data can be obtained from the CIF file, with the CSD number 1981899, freely available at the Cambridge Crystallographic Data Center [17].

The structure of RbSbGe₃O₉ is in very good agreement with that proposed for the room-temperature BaTiGe₃O₉ (BTG) allotropic form [6] and the high-pressure BaTiSi₃O₉ (BTS) silicate [18]. The authors have indexed the X-ray powder patterns of the BTG compound in a $P31c$ trigonal cell, $a = 11.73$ and $c = 10.02$ Å, which contains 6 formula units [6]. Regarding the high-pressure BTS polymorph, the single-crystal structure solved from X-ray data is also described with $Z = 6$ in the $P31c$ space group for a lattice of dimensions $a = 11.3382(9)$ and $c = 9.6584(9)$ Å [18].

Table 1. Main crystal data and refinement parameters for RbSbGe₃O₉.

Formula weight	568.99
Wavelength (Å)	0.71073
Space group	<i>P</i> 31 <i>c</i> , (n°159)
Temperature (K)	293 (2)
<i>a</i> (Å)	12.1378(2)
<i>c</i> (Å)	9.9553(2)
<i>V</i> (Å ³)	1270.18(5)
<i>Z</i>	6
Calculated density (Mg/m ³)	4.463
μ (mm ⁻¹)	19.44
Crystal (mm)	0.19 × 0.17 × 0.09
θ range (°)	2.818 - 49.507
Index ranges	-25 ≤ <i>h</i> ≤ 23, -25 ≤ <i>k</i> ≤ 25, -21 ≤ <i>l</i> ≤ 21
Collected reflections	49196
Independent reflections	8563 [R(int) = 0.0369]
Refined parameters	131
Goodness-of-fit on F ²	1.037
Final R indices [<i>I</i> > 2σ(<i>I</i>)]	R1 = 0.0208, wR2 = 0.0444
R indices (all data)	R1 = 0.0241, wR2 = 0.0452
Absolute structure parameter	0.030(4)
Extinction coefficient	0.0045(2)
$\Delta\rho$ Fourier residuals (e.Å ⁻³)	1.37 / -1.02

Table 2. Atomic positions and equivalent displacement parameters (Å² × 10³) for RbSbGe₃O₉.

U_{eq} is defined as 1/3 of the trace of the orthogonalized U_{ij} tensor.

	<i>x</i>	<i>y</i>	<i>z</i>	U_{eq}
Sb	0.3346(1)	0.3310(1)	0.5164(1)	4(1)
Ge(1)	0.1267(1)	0.2936(1)	0.2595(1)	5(1)
Ge(2)	0.1668(1)	0.3749(1)	0.7691(1)	5(1)
Ge(3)	0.5398(1)	0.4995(1)	0.7739(1)	5(1)
Rb(1)	0	0	-0.0108(1)	16(1)
Rb(2)	0.66667	0.33333	0.5322(1)	21(1)
Rb(3)	0.33333	0.66667	0.5292(1)	22(1)
O(1)	0.1677(2)	0.2483(2)	0.1107(3)	13(1)
O(2)	0.3867(2)	0.4728(2)	0.1467(3)	12(1)
O(3)	0.2672(3)	0.4246(3)	0.9062(3)	19(1)
O(4)	0.4248(3)	0.4979(2)	0.4286(3)	12(1)
O(5)	0.6285(2)	0.5138(2)	0.2633(4)	11(1)
O(6)	0.2527(3)	0.4044(3)	0.6210(3)	17(1)

O(7)	0.1939(3)	0.2577(3)	0.3906(3)	20(1)
O(8)	0.1507(2)	0.4477(2)	0.2648(4)	12(1)
O(9)	0.0379(2)	0.2228(2)	0.7828(3)	9(1)

The crystal structure of $\text{RbSbGe}_3\text{O}_9$ can be considered as composed of Ge_3O_9 units linked through octahedrally coordinated Sb atoms (Sb-O distances in the range 1.937(3) - 1.962(3) Å) to form a three-dimensional network. The Diamond [19] drawing given in Figure 2 represents the 3-D network viewed as SbO_6 coordination polyhedra and GeO_4 regular tetrahedra linked by corner-sharing. The Rb atom is surrounded by six oxygen atoms at distances ranging from 2.914(3) to 2.987(3) Å and it is located in the channels of the network. The Ge-O distances range from 1.707(3) to 1.775(2) Å with an average value of 1.740 Å. The O-Ge-O angles vary from 102.36(14) ° to 116.42(16) ° with an average value of 109.21°. Some selected bond distances and angles are given in Table 3.

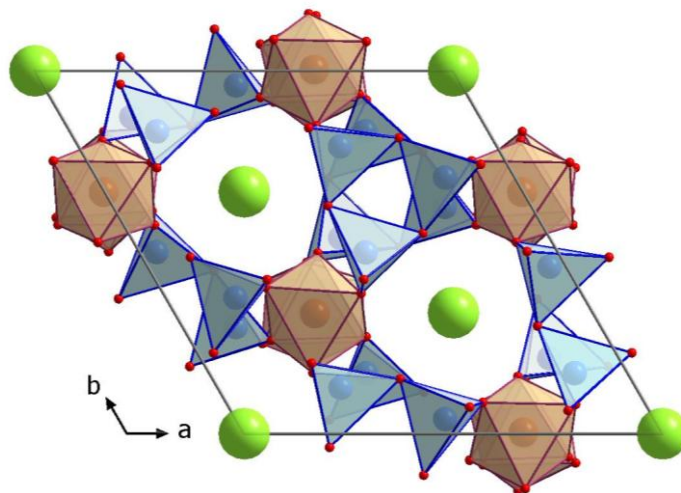


Figure 2. Projection of the structure of $\text{RbSbGe}_3\text{O}_9$ ($P31c$, $a = 12.1378$, $c = 9.9553$ Å), GeO_4 tetrahedra in blue, SbO_6 octahedra in brown and Rb^+ ions in green.

Table 3. Selected bond length and angles for RbSbGe₃O₉ crystal. The standard deviation is given in parenthesis.

Bond distances (Å)		Angles (°)	
Sb-O(6)	1.937(3)	O(6)-Sb-O(7)	91.25(12)
Sb-O(7)	1.938(3)	O(6)-Sb-O(2)#1	91.89(13)
Sb-O(2)#1	1.954(3)	O(7)-Sb-O(2)#1	173.96(8)
Sb-O(1)#1	1.957(2)	O(6)-Sb-O(1)#1	94.01(11)
Sb-O(3)#2	1.960(3)	O(7)-Sb-O(1)#1	86.70(11)
Sb-O(4)	1.962(3)	O(2)#1-Sb-O(1)#1	87.95(10)
		O(6)-Sb-O(3)#2	176.47(12)
		O(7)-Sb-O(3)#2	89.67(14)
		O(2)#1-Sb-O(3)#2	87.50(9)
		O(1)#1-Sb-O(3)#2	89.44(11)
		O(6)-Sb-O(4)	85.10(8)
		O(7)-Sb-O(4)	95.47(11)
		O(2)#1-Sb-O(4)	89.94(12)
		O(1)#1-Sb-O(4)	177.67(15)
		O(3)#2-Sb-O(4)	91.43(13)
Ge(1)-O(7)	1.707(3)	O(7)-Ge(1)-O(1)	108.71(14)
Ge(1)-O(1)	1.738(3)	O(7)-Ge(1)-O(8)	113.97(17)
Ge(1)-O(8)	1.744(2)	O(1)-Ge(1)-O(8)	116.42(16)
Ge(1)-O(9)#3	1.775(2)	O(7)-Ge(1)-O(9)#3	102.36(14)
		O(1)-Ge(1)-O(9)#3	105.68(13)
		O(8)-Ge(1)-O(9)#3	108.44(11)
Ge(2)-O(3)	1.726(3)	O(3)-Ge(2)-O(9)	114.49(16)
Ge(2)-O(9)	1.728(2)	O(3)-Ge(2)-O(6)	110.72(15)
Ge(2)-O(6)	1.736(3)	O(9)-Ge(2)-O(6)	114.67(15)
Ge(2)-O(5)#4	1.756(3)	O(3)-Ge(2)-O(5)#4	102.68(15)
		O(9)-Ge(2)-O(5)#4	110.04(11)
		O(6)-Ge(2)-O(5)#4	102.90(15)
Ge(3)-O(4)#1	1.729(3)	O(4)#1-Ge(3)-O(2)#1	109.69(13)
Ge(3)-O(2)#1	1.740(3)	O(4)#1-Ge(3)-O(5)#1	112.70(16)

Ge(3)-O(5)#1	1.749(3)	O(2)#1-Ge(3)-O(5)#1	115.97(15)
Ge(3)-O(8)#5	1.753(2)	O(4)#1-Ge(3)-O(8)#5	102.71(15)
		O(2)#1-Ge(3)-O(8)#5	104.38(16)
		O(5)#1-Ge(3)-O(8)#5	110.23(11)
Rb(1)-O(1) (3x)	2.924(2)		
Rb(1)-O(7)#6 (3x)	2.987(3)		
Rb(2)-O(3)#6 (3x)	2.914(3)		
Rb(2)-O(2)#7 (3x)	2.963(3)		
Rb(3)-O(4)#8 (3x)	2.951(3)		
Rb(3)-O(6) (3x)	2.968(3)		

Symmetry transformations used to generate the equivalent atoms:

#1 $y, x, z+1/2$; #2 $y, x, z-1/2$; #3 $-x, -x+y, z-1/2$; #5 $-x+y, -x, z$; #4 $x-y, -y+1, z+1/2$;
 #5 $x-y+1, -y+1, z+1/2$; #6 $-x+1, -x+y, z-1/2$; #7 $-x+1, -x+y, z+1/2$; #8 $-x+y, -x+1, z$

The Ge_3O_9 unit made of GeO_4 tetrahedra and involving three independent Ge atoms four-fold coordinated by oxygen is represented in Figure 3. The germanium and oxygen atoms forming the Ge_3O_3 central ring are nearly coplanar as indicated by the small deviations of their fitted positions from the mean ab plan (maximal distance to plan is $\pm 0.1 \text{ \AA}$), Figure 2. The unit cell of $\text{RbSbGe}_3\text{O}_9$ contains two sheets of Ge_3O_3 rings approximately located at $z = 0.25$ and $z = 0.75$ along the c -axis (9.95 \AA). In agreement with the symmetry of the $P31c$ space group, the Ge_3O_9 units (and Ge_3O_3 central rings) in the cell conform to the three-fold symmetry instead of the six-fold symmetry described for the benitoite-type structure within the $P\bar{6}c2$ space group [20]. A distortion of the Ge_3O_3 ring arising from the weaker symmetry of the trigonal space group causes variations in the O-Ge-O angles involving the out-of-plane oxygen atoms. It has been shown that this kind of distortion would be an inhibitor of the appearance of the benitoite-type structure characterized by Ge_3O_3 planar cycles [21, 22]. However, the structure of $\text{RbSbGe}_3\text{O}_9$ resembles that of benitoite with the presence of both isolated SbO_6 octahedra and Ge_3O_9 cyclic units but is not isostructural due to small deviations of symmetry leading to both different space groups and unit cells. It should be noticed that some germanate as RbXGe_3O_9 with $\text{X} = \text{Ta}^{\text{V}}$ or Nb^{V} were found to crystallize in the hexagonal $P\bar{6}c2$ space group

with the benitoite-type structure [7]. Therefore, it seems that the existence of the benitoite structure depends on the nature of the element X^V , and more precisely, on its size when coordinated by six oxygen atoms [7].

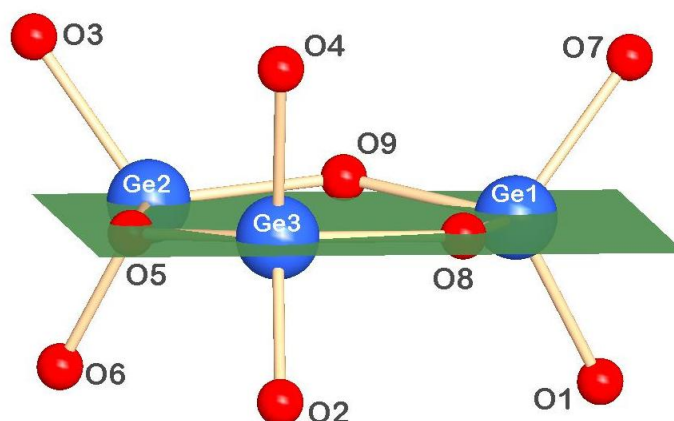


Figure 3: Representation of the Ge_3O_9 cyclic unit in $\text{RbSbGe}_3\text{O}_9$ formed with an almost planar Ge_3O_3 central ring. The atoms are labelled according to numbers in Table 3 and the mean plane (approximately ab plane) is drawn in green.

3.3 Optical characterization

The transmitted infrared (IR) and the Raman spectra, both recorded at room-temperature, for the new non-centrosymmetric $\text{RbSbGe}_3\text{O}_9$ material are presented in Figure 2. In the area of valence frequency $500\text{-}1000\text{ cm}^{-1}$, the fingerprint of our IR spectrum is consistent with a previously published work [21] and the most characteristic IR band of a Ge_3O_3 planar ring is immediately identified at 566 cm^{-1} , Figure 4a. It has been reported for the germanates of benitoite-type that this band, associated with the symmetric deformation vibration $\nu_s(\text{GeOGe})$, is unique as long as the Ge_3O_3 ring has the local D_{3h} high symmetry and splits into a multiplet for a distorted ring [21, 22]. No splitting is observed for this high-intensity “ring IR band” in the infrared spectrum of $\text{RbSbGe}_3\text{O}_9$, this is consistent with the single-crystal structure

determination as the deviation of Ge and O atom positions from the mean plane of the Ge_3O_3 ring is very small (max. $\pm 0.1 \text{ \AA}$).

The non-polarized Raman scattering spectrum, Figure 4b, registered for a single crystal platelet of $\text{RbSbGe}_3\text{O}_9$ using a 473 nm laser line is in agreement with the earlier published spectrum collected at 632.8 nm on a powdered sample [21]. It can be divided into 3 parts: the low-wavenumber domain $[100\text{-}350] \text{ cm}^{-1}$, the middle range $[400\text{-}650] \text{ cm}^{-1}$ and the high-frequency zone $[750\text{-}950] \text{ cm}^{-1}$. The mid-range is particularly interesting because this is the domain where the bands associated with “ring vibrations” appear. The strong Raman bands centered at 489 and 523 cm^{-1} can be assigned to the symmetric stretching of Ge-O-Ge in the Ge_3O_9 cycle as it has already been reported [10].

The IR and Raman results are both consistent with the presence of Ge_3O_9 units in the $\text{RbSbGe}_3\text{O}_9$ structure and with the almost perfect planarity of the Ge_3O_3 central ring.

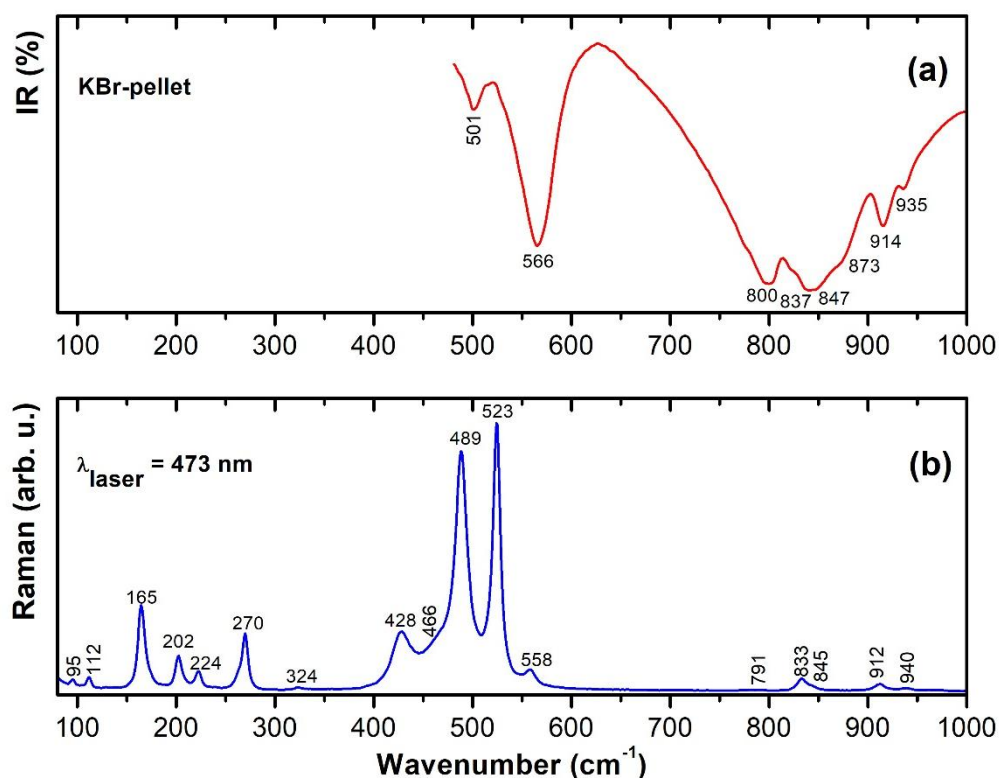


Figure 4: Unpolarized infrared (a) and Raman (b) spectra registered at room-temperature for RbSbGe₃O₉ samples.

4. CONCLUSION

A new colorless and transparent germanate has been obtained as single-crystals by the flux method. It is thermally stable up to its melting point at 1061°C and it is not air-sensitive. The room-temperature RbSbGe₃O₉ structure, solved and refined in the non-centrosymmetric space group *P31c*, even if not isostructural, is comparable to the benitoite-type in terms of polyhedral content, with the coexistence of SbO₆ isolated octahedra and Ge₃O₉ cyclic units. The slight deviation in the *z*-position of atoms that form the Ge₃O₃ ring is responsible for lowering of the space group symmetry but it is not significant enough to affect the vibrational “ring band” characteristics as shown by IR and Raman spectroscopy. The RbSbGe₃O₉ germanate is isostructural to the BaTiGe₃O₉ room-temperature allotrope and to the high-pressure BaTiSi₃O₉ silicate.

This oxide material which displays a large thermal stability range may have piezo-electrical and non-linear optical properties, even at elevated temperatures. Therefore, larger single-crystals must be obtained to determine if this material is anisotropic and changes properties with direction.

Acknowledgment

The EDX experiments were conducted at the Plateau Technique Microscopie à Balayage at the IEM Institute in Montpellier, France. IR, Raman and single-crystal X-ray diffraction

experiments were done at Platform of Analysis and Characterization of the Pôle Chimie Balard in Montpellier, France.

REFERENCES

[1] Top-Seeded Solution Growth and Structural Characterizations of α -Quartz-like Structure GeO_2 Single Crystal.

A. Lignie, B. Ménaert, P. Armand, A. Peña, J. Debray, P. Papet
Cryst. Growth Des. 13 (2013) 4220-4225.

[2] High-temperature piezoelectric properties of flux-grown α - GeO_2 single crystal.

P. Papet, M. Bath, A. Haidoux, B. Ruffle, B. Menaert, A. Peña, J. Debray, P. Armand
J. Appl. Phys. 126 (2019) 144102.

[3] Density Functional Theory Predictions of the Nonlinear Optical Properties in α -Quartz-type Germanium Oxide.

P. Hermet, G. Fraysse, A. Lignie, P. Armand and Ph. Papet
J. Phys. Chem. C 116 (2012) 8692-8698.

[4] Modulation of quartz-like GeO_2 structure by Si substitution: an X-ray diffraction study of $\text{Ge}_{1-x}\text{Si}_x\text{O}_2$ ($0 \leq x < 0.2$) flux-grown single-crystals.

A. Lignie, D. Granier, P. Armand, J. Haines and P. Papet
J. Appl. Cryst. 45 (2012) 272-278.

[5] Crystal Structure of $\text{BaGe}[\text{Ge}_3\text{O}_9]$ and its Relation to Benitoite.

C. Robbins, A. Perloff, S. Block
J. Res. Natl. Bur. Stand. 70A (1966) 385-391.

[6] The Compound $\text{BaTiGe}_3\text{O}_9$

R. Robbins
J. Am. Ceram. Soc. 43(11) (1960) 610-610.

[7] Sur de nouveaux germanates et silicates de type Bénitoïte.

J. Choisnet, A. Deschanvres, B. Raveau

J. Solid State Chem. 4 (1972) 209-2018.

[8] Synthèse et évolution structurale de nouveaux silicogermanates $\text{BaGe}(\text{Ge}_{3-x}\text{Si}_x)\text{O}_9$ de type benitoïte et de structure apparentée.

M. Goreaud, J. Choisnet, A. Deschanvres, B. Raveau

Mat. Res. Bull. 8 (1973) 1205-1214.

DOI: 10.1016/0025-5408(73)90158-X

[9] A potential red-emitting Phosphor $\text{BaZrGe}_3\text{O}_9:\text{Eu}^{3+}$ for WLED and FED applications: Synthesis, structure and luminescence properties.

Q. Zhang, X. Wang, X. Ding, Y. Wang

Inorg. Chem. 56 (2017) 6990-6998.

DOI: 10.1021/acs.inorgchem.7b00591

[10] Raman spectroscopic study of benitoite-type compounds.

Y. Takahashi, K. Iwasaki, H. Masai, T. Fujiwara

J. Ceram. Soc. Jpn. 116 (2008) 1139-1142.

[11] Phase-stability and photoluminescence of $\text{BaTi}(\text{Si}, \text{Ge})\text{O}_3$.

Y. Takahashi, K. Kitamura, N. Iyi, S. Inoue

J. Ceram. Soc. Jpn 114 (2006) 313-317

DOI: 10.2109/jcersj.114.313

[12] APEX3. Version 2017.3-0, Bruker AXS, Inc., Madison, Wisconsin, USA, 2017

[13] Crystal structure refinement with *SHELXL*

G. M. Sheldrick

Acta Cryst. C71 (2015) 3-8

<https://doi.org/10.1107/S2053229614024218>

[14] SHELXT - Integrated space-group and crystal-structure determination

G. M. Sheldrick

Acta Cryst. A71 (2015) 3-8
<https://doi.org/10.1107/S2053273314026370>

[15] The joint Committee on Powder Diffraction Standards Card N° 00-027-0524.

[16] JANA2006
V. Petricek, M. Dusek, L. Palatinus
Z. Kristallogr. 229(5) (2014) 345-352.

[17] <http://www.ccdc.cam.ac.uk/conts/retrieving.html> (or from the CCDC, 12 Union Road, Cambridge CB2 1EZ, UK; Fax: +44 1223 336033; E-mail: deposit@ccdc.cam.ac.uk).

[18] Second-order *P*-6*c*2-*P*31*c* transition and structural crystallography of the cyclosilicate benitoite, BaTiSi₃O₉, at high pressure.
C. Hejny, R. Miletich, A. Jasser, P. Schouwink, W. Crichton, V. Kahlenberg
Am. Mineral. 97 (2012) 1749-1763.

[19] Diamond - Crystal and Molecular Structure Visualization
Crystal Impact - Dr. H. Putz & Dr. K. Brandenburg GbR, Kreuzherrenstr. 102, 53227 Bonn, Germany
<http://www.crystalimpact.com/diamond>

[20] The Crystal Structure of Benitoite, BaTiSi₃O₉
W. H. Zachariasen
Z. Kristallogr. Cryst. Mater 74 (1930) 139–146.

[21] Spectres vibrationnels des silicates et germanates renfermant des anneaux, M₃O₉ (M=Si, Ge)-I. Attribution des fréquences caractéristiques de l'anneau M₃O₉ dans les composés de type bénitoïte, wadéïte et tétragermanate.
J. Choisnet, A. Deschanvres, P. Tarte
Spectrochim. Acta A 31 (1975) 1023-1034.

[22] Spectres vibrationnels des silicates et germanates renfermant des anneaux, M₃O₉ (M=Si, Ge)-II. Etude des spectres vibrationnels des silicogermanates de type bénitoïte : mise en évidence des anneaux mixtes (GeSi₂O₉) et (Ge₂SiO₉).
J. Choisnet, A. Deschanvres, P. Tarte
Spectrochim. Acta A 32 (1976) 57-66.

